Characterization of linear viscoelastic, nonlinear viscoelastic and damage stages of asphalt mixtures[1]

Rong Luo, Ph.D., P.E.
Professor
School of Transportation
Wuhan University of Technology
1178 Heping Avenue
Wuhan, Hubei Province 430063, China
Phone: +86 (27) 8653 1551
Fax: +86 (27) 8653 1551
Email: rongluo@whut.edu.cn

Hanqi Liu, Ph.D. Candidate
Graduate Research Assistant
School of Transportation
Wuhan University of Technology
1178 Heping Avenue
Wuhan, Hubei Province 430063, China
Phone: +86 (27) 8653 1551
Fax: +86 (27) 8653 1551
Email: hanqiliu@whut.edu.cn

Yuqing Zhang, Ph.D.
Lecturer
School of Engineering and Applied Science
Aston University
MB153A, Aston Triangle
Birmingham, B4 7ET, U.K.
Phone: +44 (0) 121-204-3391
Email: y.zhang10@aston.ac.uk

[1] This is an Accepted Manuscript of an article published by Elsevier in *Construction and Building Materials*. The final publication is available online via http://doi.org/10.1016/j.conbuildmat.2016.08.039

Abstract

It has been demonstrated that asphalt mixtures experienced linear viscoelastic stage, nonlinear viscoelastic stage and damage stage when subjected to controlled-strain repeated direct-tension (RDT) tests with increasing strain levels. However, the linear viscoelastic properties of asphalt mixtures are usually muddled up with their nonlinear viscoelastic properties. These confusions directly lead to the incorrect determination of the pseudostrains and dissipated pseudostrain energies (DPSEs) in the nonlinear viscoelastic stage and damage stage. This study investigated the material properties of fine aggregate mixture (FAM) specimens in all three stages. These three stages were differentiated and characterized in terms of the viscoelastic stress, pseudostrain and DPSE. The definitions of viscoelastic stress, reference modulus and pseudostrain were rigorously established to assure that the material properties in the linear viscoelastic stage were the reference properties and that the sole linear viscoelastic effect was eliminated when determining the pseudostrain and DPSE in the three stages. The characteristics of the DPSE in the three stages were found to be: 1) the DPSE of any loading cycle was zero in the linear viscoelastic stage; 2) in the nonlinear viscoelastic stage, the DPSE of each loading cycle remained approximately the same with the growth of the number of loading cycles, and the DPSE increased to a larger value when the strain level of the RDT test increased to a higher level; 3) in the damage stage, the DPSE of the loading cycle increased as the number of loading cycles increased. This study strictly distinguished the linear viscoelasticity from the nonlinear viscoelasticity of the asphalt mixtures, which is critical for the accurate determination of the DPSE spent in overcoming the nonlinear viscoelasticity and in developing damages, such as cracking and permanent deformation, in the asphalt mixtures.

Keywords:

Asphalt mixture; linear viscoelasticity; nonlinear viscoelasticity; viscoelastic stress; pseudostrain; dissipated pseudostrain energy.

1. Introduction

Paving asphalt mixtures are complex composite materials that may exhibit different properties at different strain levels. It has been demonstrated that, when subjected to typical controlled-strain repeated direct-tension (RDT) tests, an asphalt mixture experiences multiple stages as the strain level increases, which include: 1) undamaged stage, consisting of the linear viscoelastic stage and the nonlinear viscoelastic stage; and 2) damage stage [1][2]. These stages have the following characteristics:

(1) Undamaged stage:

a. At any specific strain level, the material properties stay constant despite of the increase of the number of loading cycles;
b. The deformation of the asphalt mixture is completely recovered after unloading;
c. As the strain level varies, the asphalt mixture has different properties in the linear viscoelastic stage from those in the nonlinear viscoelastic stage:
    i. Linear viscoelastic stage: the material properties remain unchanged if the strain level varies within this stage;
    ii. Nonlinear viscoelastic stage: the material properties change as the strain level varies;

(2) Damage stage:

a. At any specific strain level, the material properties vary with the increase of the number of loading cycles;
b. The deformation of the asphalt mixture cannot be completely recovered after unloading; and
c. The material properties change as the strain level varies.

If using the pseudostrain defined in Equation 1 to eliminate the linear viscoelastic effect [3], these stages can be illustrated via the stress-pseudostrain curve, as shown in Figure 1.

$$\varepsilon_R = \frac{\sigma_{VE}(t)}{E_R} = \frac{\int_0^t E(t-\tau)\frac{\partial \varepsilon(\tau)}{\partial \tau} d\tau}{E_R} \qquad (1)$$

where ε_R = pseudostrain, με; $\sigma_{VE}(t)$ = viscoelastic stress corresponding to the measured strain history, Pa; E_R = reference modulus, MPa; t = loading time, s; τ = a dummy variable, indicating any arbitrary time between 0 and t, s; $E(t)$ = relaxation modulus in the linear viscoelastic stage, MPa; and $\varepsilon(t)$ = measured strain history, με.

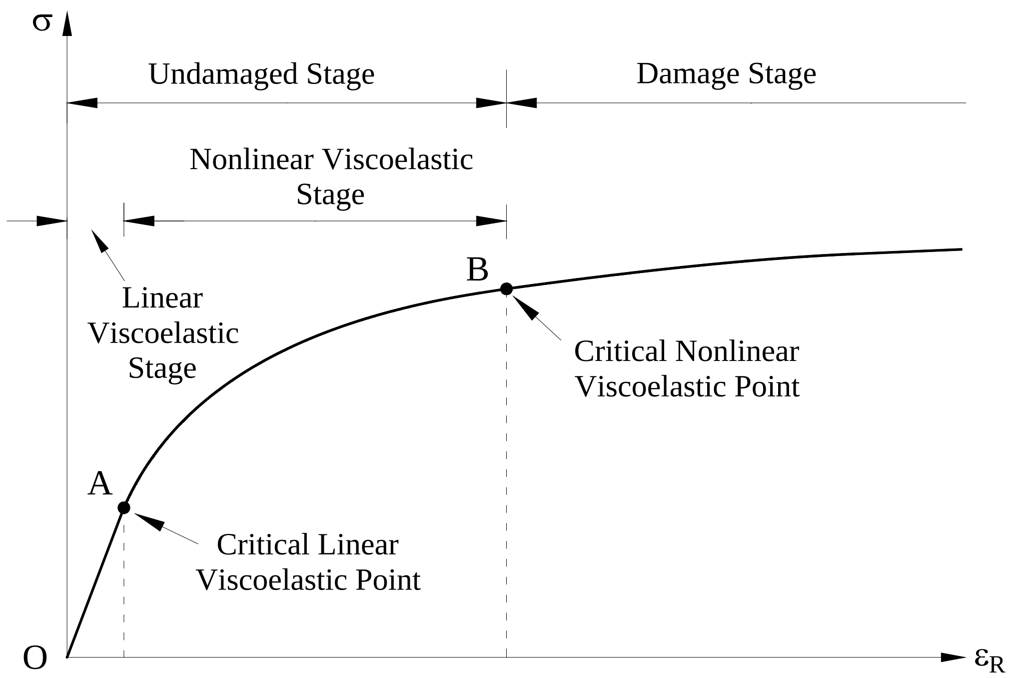

Figure 1 Stress-pseudostrain curve of an asphalt mixture in controlled-strain RDT tests (after [1][2])

Based on the identification of these distinct stages, testing to determine the mechanical properties of asphalt mixtures is made simpler and more precise by using pseudostrain concepts in analyzing the test data. However, these advantages are diminished or even lost if the analysis does not make clear distinctions and boundaries between these stages. In fact, the nonlinear viscoelastic properties are usually muddled up with the linear viscoelastic properties [1][2][4][5]. For example, $\sigma_{VE}(t)$ has been considered to be the same as the measured stress in the nonlinear viscoelastic stage, and E_R has been chosen to be the magnitude of the complex modulus at the critical nonlinear viscoelastic point (Point B) shown in Figure 1 when calculating the pseudostrain in the nonlinear viscoelastic stage [1][2]. These confusions directly lead to the incorrect determination of the pseudostrains and pseudostrain energies in the nonlinear viscoelastic stage and in the damage stage. Using these incorrectly determined results could hardly make accurate prediction of the development of the damages in the asphalt mixture, such as the fatigue cracking and permanent deformation, which are driven by the corresponding dissipated pseudostrain energies (DPSEs). As a result, there is an urgent need to rigorously determine the nonlinear viscoelastic properties of the asphalt mixture in typical controlled-strain RDT tests and to characterize the associated DPSEs in the nonlinear viscoelastic stage and damage stage.

To address this research need, this study employed a Dynamic Mechanical Analyzer (DMA) to perform controlled-strain RDT tests on fine aggregate mixture (FAM) specimens in order to investigate their material properties in the linear viscoelastic stage, nonlinear viscoelastic stage and damage stage. The DPSEs in these stages were also characterized for future applications to the prediction of the damage development in asphalt mixtures. The next section describes the configuration and procedure of the controlled-strain RDT tests. The subsequent section presents the determination of the asphalt mixture properties in different stages based on the test data. The following section details the differentiation and characterization of the linear viscoelastic stage, nonlinear viscoelastic stage and damage stage in terms of the viscoelastic stress, pseudostrain and DPSE. The final section summarizes the major findings of this study and briefs the authors' ongoing research on this subject.

2. Configuration and procedure of the controlled-strain RDT tests

2.1. Specimen fabrication

FAM specimens for the controlled-strain RDT tests were fabricated in the laboratory using an unmodified #70 petroleum asphalt binder (graded based on the penetration) and fine limestone aggregates passing No. 16 sieve with the opening of 1.18 mm. The gradation of the fine aggregates is listed in Table 1. The asphalt binder content was calculated to be 8.97% by weight of aggregates using the aggregate surface area method with the optimum asphalt content of the corresponding full asphalt mixture [6]–[9].

Table 1 Gradation of the fine aggregates in FAM specimens

Sieve No.	No. 16	No. 30	No. 50	No. 200	PAN (-No. 200)
Sieve Size (mm)	1.18	0.60	0.30	0.75	<0.075
Individual Retaining (%)	0	44.23	23.46	18.85	13.46

The procedure of fabricating and preparing the FAM specimens for testing was composed of five major steps as follows:

(1) Mixing and compaction: the aggregate batch was mixed with the asphalt binder at the temperature of 135°C; after being cured at 121°C for 2 hours, the asphalt mixture was compacted using the Superpave Gyratory Compactor (SGC) into a cylindrical raw specimen 150 mm in diameter and 70 mm in height, as shown in Figure 2(a);

(2) Cutting: the upper and lower part of the raw specimen were cut off using an automatic saw into a shorter specimen 40 mm in height, as presented in Figure 2(b);

(3) Coring: the shorter specimen were cored following the pattern illustrated using red circles in Figure 2(c) to obtain cylindrical specimens to be tested, which were 12 mm in diameter and 40 mm in height; Figure 2(d) shows an example of the FAM specimen;

(4) Gluing: each end of a FAM specimen was glued to an end platen using a 2 ton epoxy with the aid of a specially designed gluing jig, as presented in Figure 2(e), to assure the vertical pedestals of the two end platens were aligned; Figure 2(f) presents an example of the test specimen glued to end platens; and

(5) Curing: all specimens with end platens were cured in an environmental chamber at the temperature of 20°C for at least 1 hour to achieve the temperature equilibrium; the specimens were therefore ready for testing.

(a) Raw specimen

(b) Shorter specimen after cutting

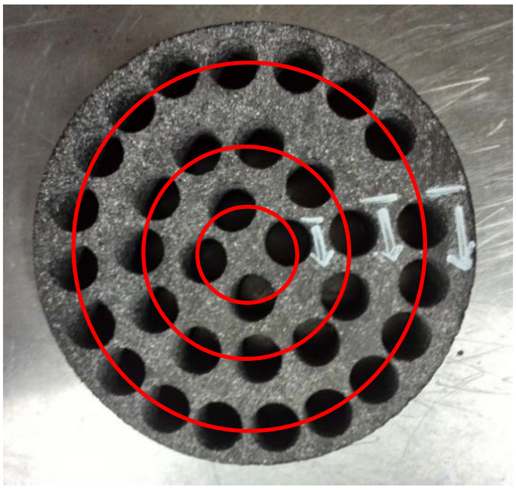

(c) Making cores

(d) FAM specimen

(e) Gluing jig

(f) Glued specimen for testing

Figure 2 Procedure of fabricating and preparing FAM specimens for testing

2.2. Test configuration

The controlled-strain RDT tests were performed on the FAM specimens using the DMA, as shown in Figure 3. Before the test, the test specimen with end platens was mounted on the upper and lower tension fixtures that were attached to the DMA (see Figure 4). As the specimen was in place, the environmental chamber was closed, which was able to control the test temperature in a range from −60°C to 600°C. The test temperature in this study was 20°C. The test protocol was programmed in the software TRIOS designed specifically for the DMA.

Figure 3 Overview of Dynamic Mechanical Analyzer (DMA)

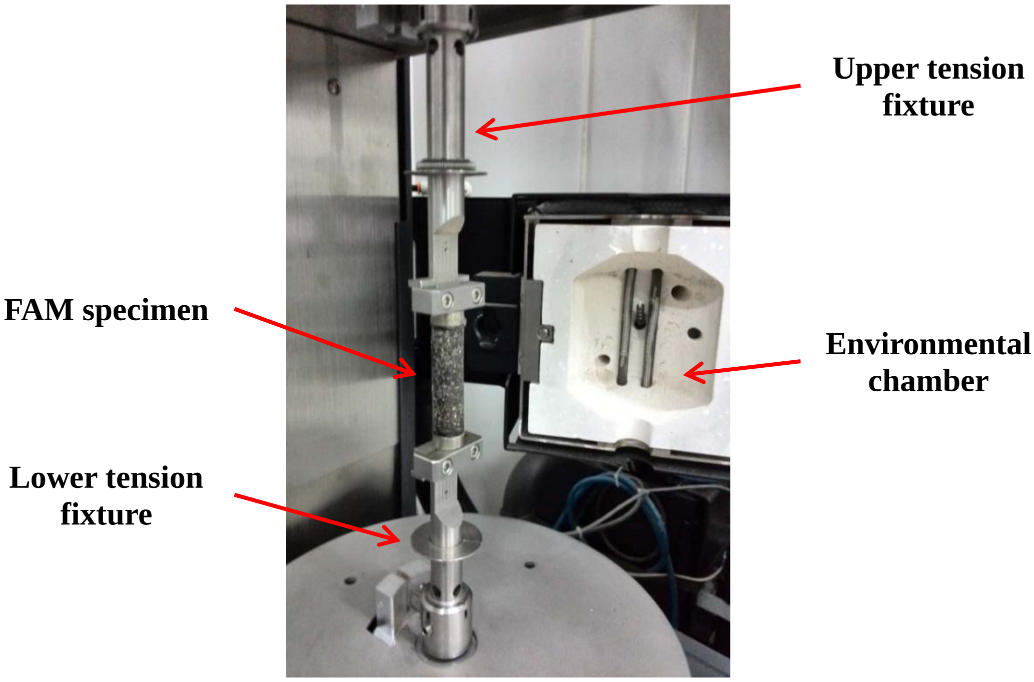

Figure 4 Configuration of DMA tests

2.3. Test procedure

The entire test procedure consisted of a sequence of consecutive controlled-strain RDT tests at different strain levels, as illustrated in Figure 5. A haversine strain curve was imposed on the specimen in each RDT test, which had 600 loading cycles with a loading frequency of 2π rad/s (1 Hz). There was a 900 s (15 min) rest period between two adjacent RDT tests in order to recover possible deformation in the previous RDT test [1][2].

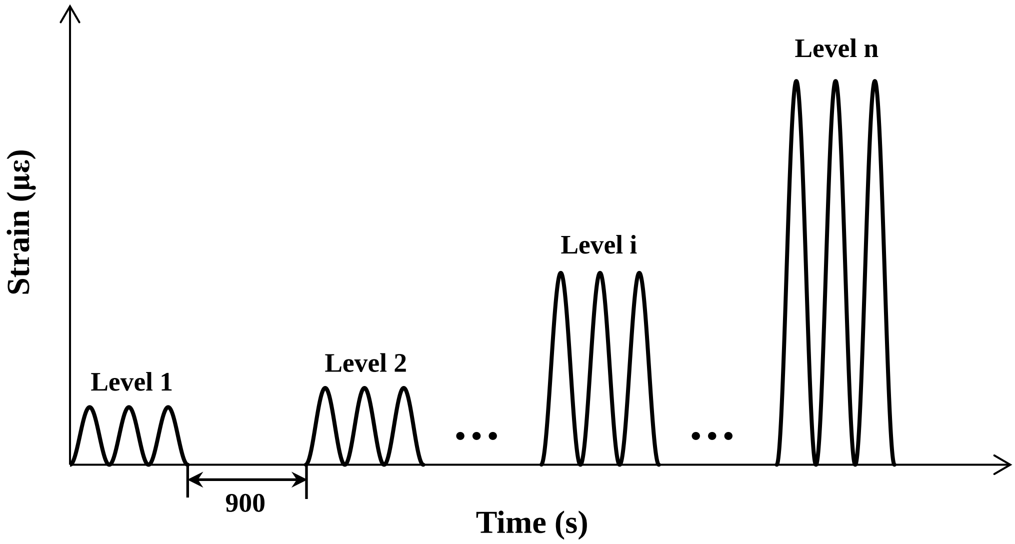

Figure 5 Controlled-strain RDT test protocol

The test protocol was designed as follows:

(1) First RDT test: the initial strain level (Level 1) of the first RDT test was selected to be 20 με to assure that the specimen was within the linear viscoelastic stage;

(2) Subsequent RDT tests from Strain Level 2 to $(n-1)$: the axial strain level was increased with an increment of 10 με until the specimen developed into the damage stage; Strain Level $(n-2)$ corresponded to the critical nonlinear viscoelastic point; and

(3) Final RDT test: the final strain level (Level *n*) was chosen to be 200 με for the purpose of introducing sufficient damages to the specimen.

3. Properties of test specimens in three stages

The strain and stress data measured from each RDT test were firstly processed in the software MATLAB using the Fourier series to filter possible noise [10]. The strain amplitude (ε_0) and stress amplitude (σ_0) of every loading cycle were therefore determined based on the peaks and troughs of the strain wave and stress wave, respectively, as illustrated in Figure 6. The magnitude of the complex modulus, $|E^*|$, of every cycle was then calculated to be:

$$|E^*| = \frac{\sigma_0}{\varepsilon_0} \tag{2}$$

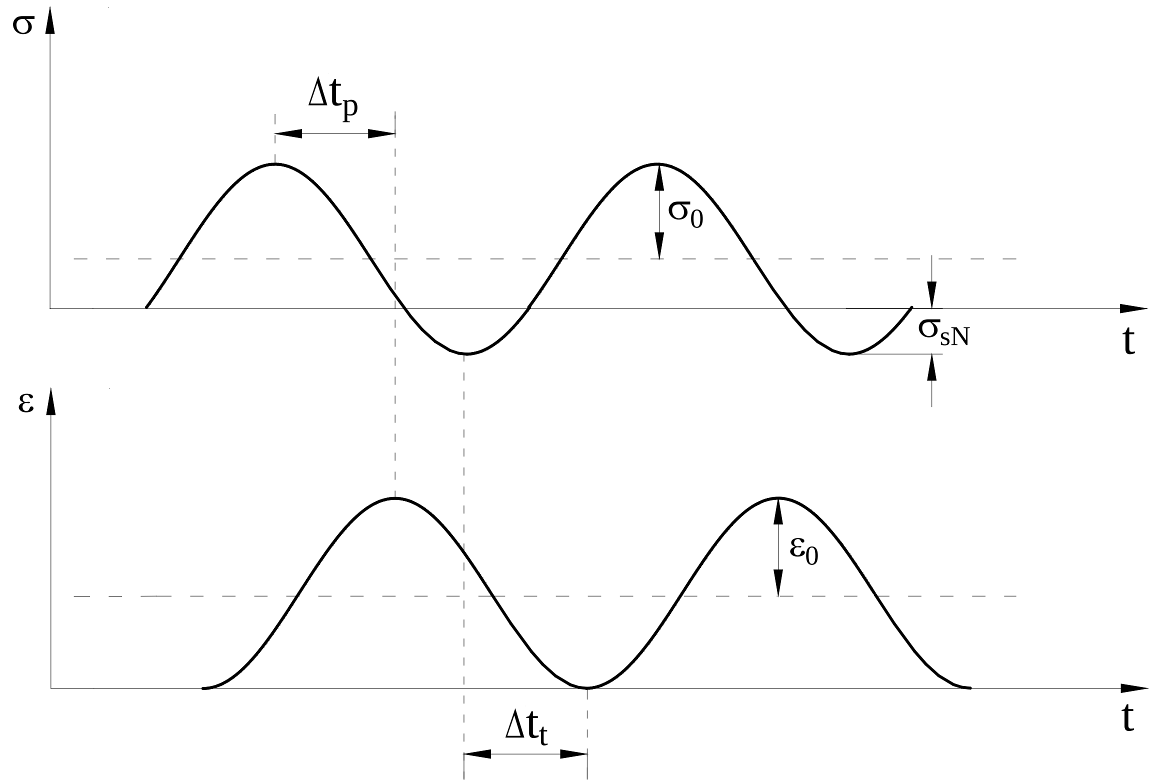

Figure 6 Stress and strain waves

To determine the phase angle of the complex modulus, φ, the time lag between the peaks and the time lag between the troughs of the strain and stress waves in the same loading cycle were identified to be Δt_p and Δt_t, respectively, as shown in Figure 6. It was found that Δt_p and Δt_t were not exactly the same in most loading cycles. Therefore, the average value of Δt_p and Δt_t was used to compute the phase angle of the complex modulus in the corresponding loading cycle as shown in Equation 3:

$$\varphi = \frac{\Delta t_p + \Delta t_t}{2} \cdot \omega \tag{3}$$

where ω = loading frequency, 2π rad/s. Examples of the determined $|E^*|$ and φ at strain levels of 30 με, 50 με, 70 με and 200 με are presented in Figure 7, in which φ is converted into degrees for the convenience of visual comparison.

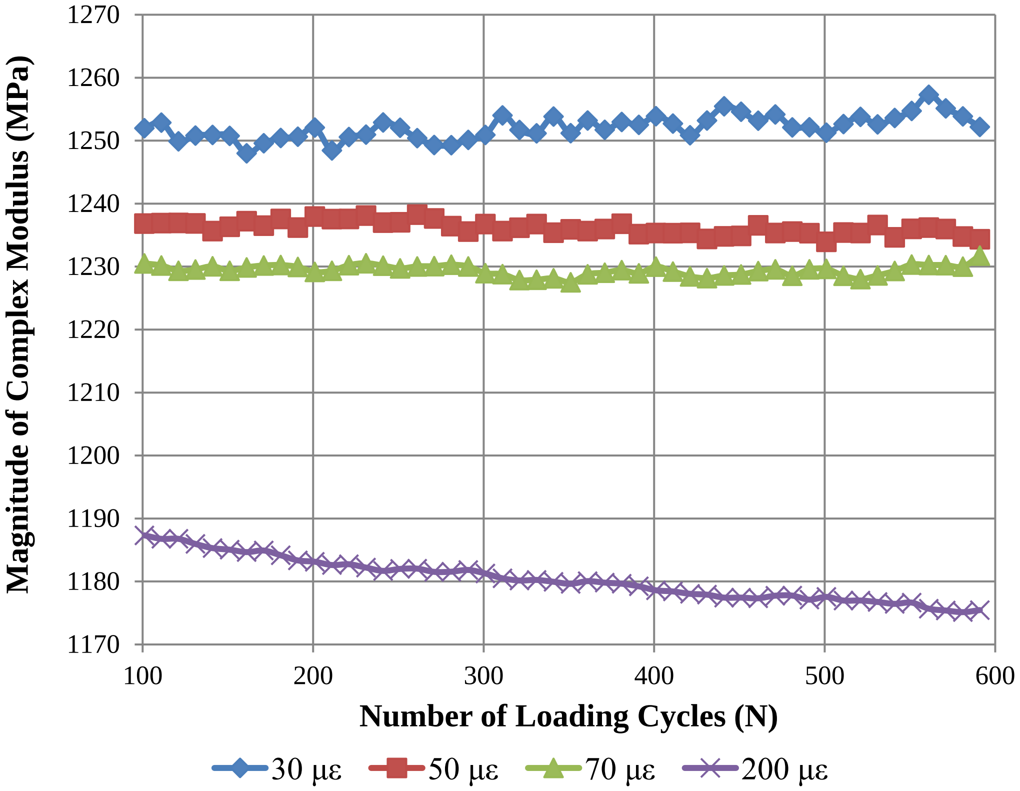

(a) Magnitude of complex modulus

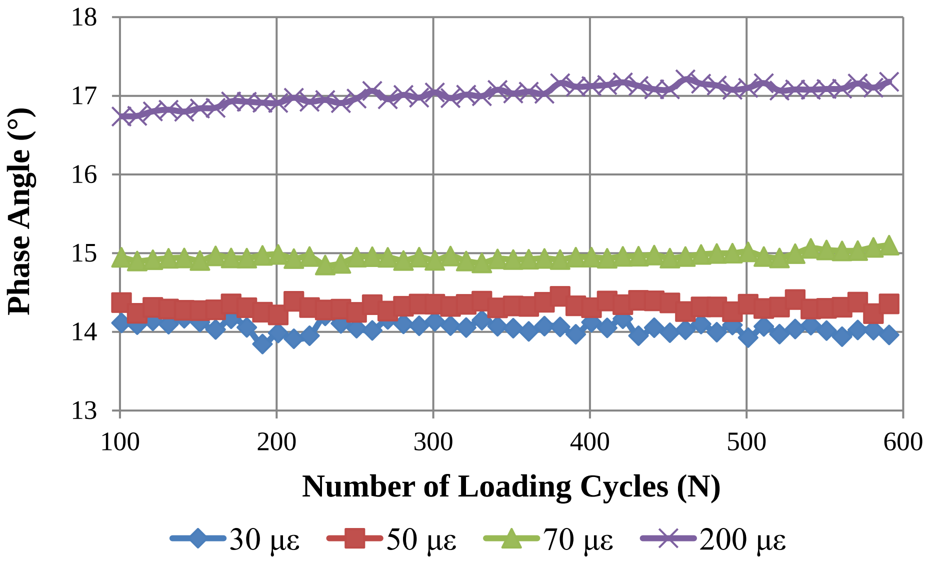

(b) Phase angle of complex modulus

Figure 7 Examples of determined magnitudes and phase angles of complex moduli

The above data analysis was applied to each RDT test starting from Strain Level 1 that was 20 με. The $|E^*|$ and φ of every loading cycle in each RDT test were therefore determined. According to their characteristics, as detailed in Introduction, the linear viscoelastic stage, nonlinear viscoelastic stage and damage stage were identified for the asphalt mixture specimens tested in this study. It was found that 30 με corresponded to the critical linear viscoelastic point (Point A in Figure 1) and 80 με corresponded to the critical nonlinear viscoelastic point (Point B in Figure 1). Based on the identification of the three stages, the viscoelastic stress, pseudostrain and DPSE will be determined in the next section.

4. Characterization of three stages

Based on the measured specimen properties and the identification of the linear viscoelastic, nonlinear viscoelastic and damage stages, these three stages were further characterized and differentiated in terms of the viscoelastic stress, pseudostrain and DPSE. First of all, the pseudostrain was rigorously defined in this study to eliminate the **linear viscoelastic** effect only. As a result, regarding the pseudo strain definition shown in Equation 1, this study considered $\sigma_{VE}(t)$ to be the linear viscoelastic stress corresponding to the measured strain history, E_R to be the magnitude of the complex modulus in the linear viscoelastic stage and $E(t)$ to be the relaxation modulus in the linear viscoelastic stage. In other words, the material properties in the **linear viscoelastic** stage were the reference properties, based on which the viscoelastic stress, pseudostrain and DPSE were calculated in all three stages as follows.

4.1. Viscoelastic stress

To determine the viscoelastic stress, the strain and stress waves measured in each RDT test were firstly simulated using Equations 4 and 5, respectively:

$$\varepsilon_m(t) = \varepsilon_0\left[1-\cos(\omega t-\varphi)\right] = \varepsilon_0 - \varepsilon_0\cos(\omega t-\varphi) \tag{4}$$

$$\sigma_m(t) = \sigma_{0N}\left[1-\cos(\omega t)\right] - \sigma_{sN} \tag{5}$$

where $\varepsilon_m(t)$ = measured strain, με; t = time, s; $\sigma_m(t)$ = measured stress, Pa; σ_{0N} = stress amplitude of the Nth loading cycle, Pa; σ_{sN} = absolute value of the downward shift of the stress curve in the Nth loading cycle, Pa. Equation 4 was then re-arranged as [2]:

$$\varepsilon_m(t) = \varepsilon_1(t) - \varepsilon_2(t) \tag{6}$$

where $\varepsilon_1(t) = \varepsilon_0$, which was a constant strain history, με; and $\varepsilon_2(t) = \varepsilon_0\cos(\omega t-\varphi)$, which was a sinusoidal strain history, με.

The viscoelastic stresses corresponding to $\varepsilon_1(t)$ and $\varepsilon_2(t)$ were determined to be:

$$\sigma_{VE1}(t)=\varepsilon_1(t)E(t)=\varepsilon_0 E(t) \tag{7}$$

$$\sigma_{VE2}(t)=\varepsilon_0 \left|E^*\right|_{LVE}\cos\left(\omega t-\varphi+\varphi_{LVE}\right) \qquad \text{(Derivation detailed in Appendix)} \tag{8}$$

where $\sigma_{VE1}(t)$ = viscoelastic stress corresponding to $\varepsilon_1(t)$, Pa; $E(t)$ = relaxation modulus in the linear viscoelastic stage, MPa; $\sigma_{VE2}(t)$ = viscoelastic stress corresponding to $\varepsilon_2(t)$, Pa; $\left|E^*\right|_{LVE}$ = magnitude of the complex modulus in the linear viscoelastic stage, MPa; φ_{LVE} = phase angle of the complex modulus in the linear viscoelastic stage, rad. Therefore, the viscoelastic stress corresponding to $\varepsilon_m(t)$ was the difference between $\sigma_{VE1}(t)$ and $\sigma_{VE2}(t)$:

$$\sigma_{VE}(t)=\varepsilon_0 E(t)-\varepsilon_0\left|E^*\right|_{LVE}\cos\left(\omega t-\varphi+\varphi_{LVE}\right) \tag{9}$$

According to the general formulation of $\sigma_{VE}(t)$ presented in Equation 9, specific formulations of $\sigma_{VE}(t)$ were established for the linear viscoelastic, nonlinear viscoelastic and damage stages, respectively:

(1) <u>Linear viscoelastic stage</u>: since φ was equal to φ_{LVE}, $\sigma_{VE}(t)$ was simplified as:

$$\sigma_{VE}(t)=\varepsilon_0 E(t)-\varepsilon_0\left|E^*\right|_{LVE}\cos(\omega t) \tag{10}$$

(2) <u>Nonlinear viscoelastic stage</u>: at a specific strain level where the phase angle was φ_{NL}, $\sigma_{VE}(t)$ was formulated as:

$$\sigma_{VE}(t)=\varepsilon_0 E(t)-\varepsilon_0\left|E^*\right|_{LVE}\cos\left(\omega t-\varphi_{NL}+\varphi_{LVE}\right) \tag{11}$$

(3) <u>Damage stage</u>: the formulation of $\sigma_{VE}(t)$ in a specific loading cycle with a phase angle of φ_D was developed as:

$$\sigma_{VE}(t)=\varepsilon_0 E(t)-\varepsilon_0\left|E^*\right|_{LVE}\cos\left(\omega t-\varphi_D+\varphi_{LVE}\right) \tag{12}$$

The above formulations of $\sigma_{VE}(t)$ will be used to determine the pseudostrain and DPSE in the following subsections.

4.2. Pseudostrain

To calculate the pseudostrains in all three stages, $E(t)$ was further derived based on the formulation of $\sigma_{VE}(t)$ in the viscoelastic stage. Since $\sigma_{VE}(t)$ and $\sigma_m(t)$ were exactly the same in the linear viscoelastic stage, Equation 13 was firstly established for the linear viscoelastic stage:

$$\sigma_{VE}\left(t\right)=\sigma_{m}\left(t\right) \tag{13}$$

According to Equation 13, $E\left(t\right)$ was then derived based on Equations 5 and 10:

$$E\left(t\right)=\left|E^{*}\right|_{LVE}-\frac{\sigma_{s,LVE}\left(t\right)}{\varepsilon_{0,LVE}} \tag{14}$$

where $\sigma_{s,LVE}\left(t\right)$ = absolute value of the downward shift of the stress curve in an RDT test in the linear viscoelastic stage, Pa; $\varepsilon_{0,LVE}$ = strain amplitude of the same RDT test, με. For a specific loading cycle in any RDT test, both $E\left(t\right)$ and $\sigma_{s,LVE}\left(t\right)$ were considered to be constants within the loading cycle. As a result, the value of $E\left(t\right)$ in the Nth loading cycle of a specific RDT test in the linear viscoelastic stage was determined to be:

$$E_{N}=\left|E^{*}\right|_{LVE}-\frac{\sigma_{sN,LVE}}{\varepsilon_{0,LVE}} \tag{15}$$

where E_{N} = the value of the relaxation modulus in the Nth loading cycle of an RDT test in the linear viscoelastic stage, MPa; and $\sigma_{sN,LVE}$ = absolute value of the downward shift of the stress curve in the Nth loading cycle of the same RDT test, Pa.

Based on the determination of the relaxation modulus, the pseudostrains in the three stages were determined using Equation 1 with the terms defined at the beginning of this section, which are detailed as follows.

(1) Linear viscoelastic stage

The pseudostrain was calculated based on Equations 1, 10 and 14:

$$\begin{aligned}\varepsilon_{R}\left(t\right)&=\frac{\sigma_{VE}\left(t\right)}{E_{R}}\\&=\frac{\varepsilon_{0}E\left(t\right)-\varepsilon_{0}\left|E^{*}\right|_{LVE}\cos\left(\omega t\right)}{\left|E^{*}\right|_{LVE}}\\&=\frac{\varepsilon_{0}\left(\left|E^{*}\right|_{LVE}-\frac{\sigma_{s,LVE}\left(t\right)}{\varepsilon_{0,LVE}}\right)-\varepsilon_{0}\left|E^{*}\right|_{LVE}\cos\left(\omega t\right)}{\left|E^{*}\right|_{LVE}}\end{aligned} \tag{16}$$

Since $\varepsilon_{0}=\varepsilon_{0,LVE}$ for a specific RDT test in the linear viscoelastic stage, Equation 17 was then established for the Nth loading cycle of the RDT test:

$$\varepsilon_{RN}(t) = \varepsilon_0\left[1 - \cos(\omega t)\right] - \frac{\sigma_{sN,LVE}}{\left|E^*\right|_{LVE}} \tag{17}$$

Comparing Equations 5 to 17 showed that $\varepsilon_R(t)$ was in phase with $\sigma_m(t)$. As a result, if plotting the measured stress versus pseudostrain, it became a straight line instead of a hysteresis loop, and this straight line passed through the origin. Figure 8 presents an example of the $\sigma_m(t)$ vs. $\varepsilon_R(t)$ graph of the 101st loading cycle of the RDT test with a strain level of 30 με. This graph demonstrated that the entire linear viscoelastic effect was successfully removed in the linear viscoelastic stage, which validated the pseudostrain formulation established in this study.

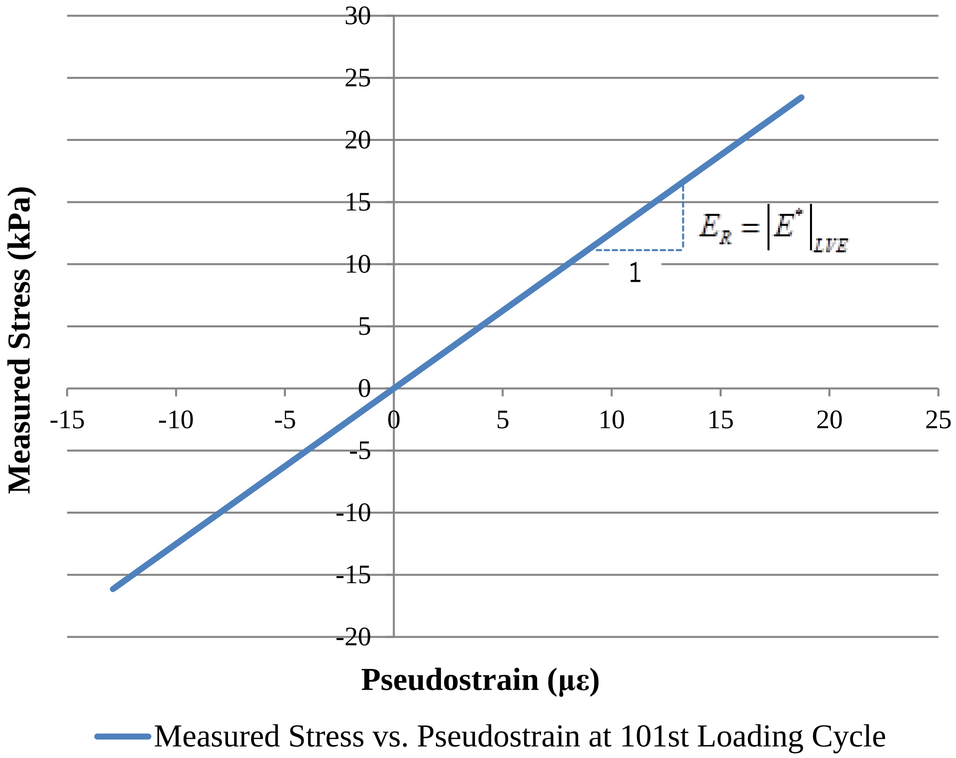

Figure 8 Measured stress vs. pseudostrain in the linear viscoelastic stage (Strain level = 30 με)

(2) Nonlinear viscoelastic stage

The pseudostrain in the nonlinear viscoelastic stage was determined based on Equations 1, 11 and 14:

$$\begin{aligned}\varepsilon_R(t) &= \frac{\sigma_{VE}(t)}{E_R} \\ &= \frac{\varepsilon_0 E(t) - \varepsilon_0 \left|E^*\right|_{LVE} \cos\left(\omega t - \varphi_{NL} + \varphi_{LVE}\right)}{\left|E^*\right|_{LVE}} \\ &= \frac{\varepsilon_0 \left(\left|E^*\right|_{LVE} - \dfrac{\sigma_{s,LVE}(t)}{\varepsilon_{0,LVE}} \right) - \varepsilon_0 \left|E^*\right|_{LVE} \cos\left(\omega t - \varphi_{NL} + \varphi_{LVE}\right)}{\left|E^*\right|_{LVE}} \\ &= \varepsilon_0 \left[1 - \cos\left(\omega t - \varphi_{NL} + \varphi_{LVE}\right)\right] - \frac{\varepsilon_0}{\varepsilon_{0,LVE}} \cdot \frac{\sigma_{s,LVE}(t)}{\left|E^*\right|_{LVE}}\end{aligned} \tag{18}$$

The pseudostrain formulation for the Nth loading cycle of an RDT test in the nonlinear viscoelastic stage was then derived as:

$$\varepsilon_{RN}(t) = \varepsilon_0 \left[1 - \cos\left(\omega t - \varphi_{NL} + \varphi_{LVE}\right)\right] - \frac{\varepsilon_0}{\varepsilon_{0,LVE}} \cdot \frac{\sigma_{sN,LVE}}{\left|E^*\right|_{LVE}} \tag{19}$$

Comparing Equations 5 to 19 indicated that $\varepsilon_R(t)$ was no longer in phase with $\sigma_m(t)$. The phase angle between $\varepsilon_R(t)$ and $\sigma_m(t)$ was $\left(\varphi_{NL} - \varphi_{LVE}\right)$, which was larger than zero since $\varphi_{NL} > \varphi_{LVE}$. In a specific RDT test in the nonlinear viscoelastic stage, $\left(\varphi_{NL} - \varphi_{LVE}\right)$ stayed unchanged as the number of loading cycles increased because of the characteristics of this stage as stated in previous sections. The $\sigma_m(t)$ vs. $\varepsilon_R(t)$ graph of any loading cycle exhibited an ellipse-shaped hysteresis loop, whose center was not located at the origin. The area of this ellipse was the DPSE spent overcoming the sole effect of the nonlinear viscoelasticity since the entire linear viscoelastic effect was eliminated already with the aid of the pseudostrain formulation. Figure 9 presents an example of the $\sigma_m(t)$ vs. $\varepsilon_R(t)$ graph at the 101st loading cycle of the RDT test with a strain level of 80 με in the nonlinear viscoelastic stage.

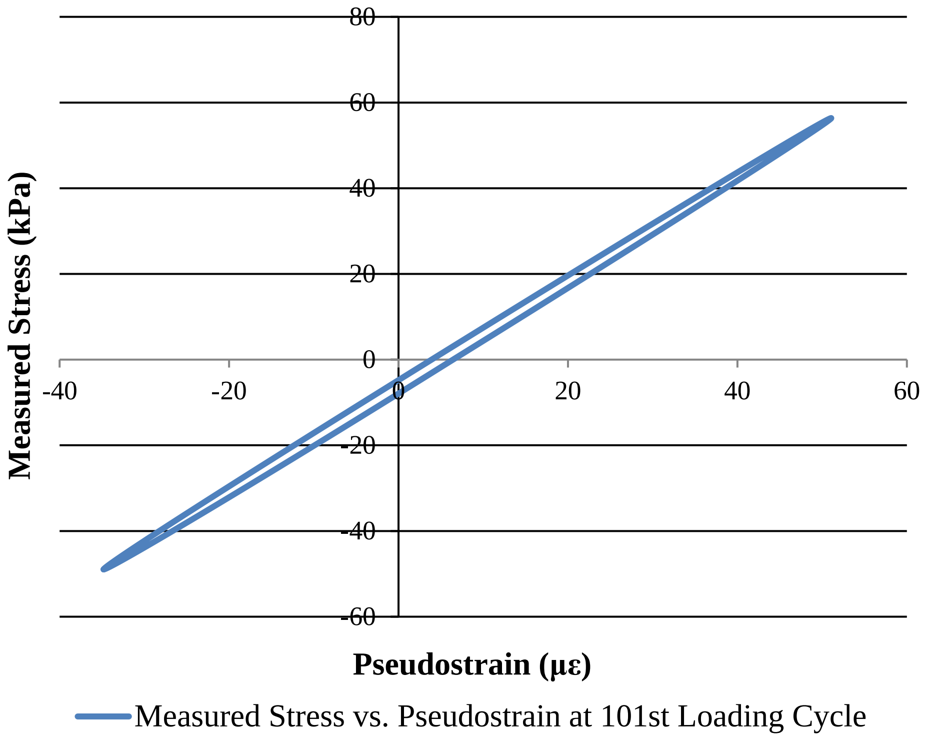

Figure 9 Measured stress vs. pseudostrain in the nonlinear viscoelastic stage (Strain level = 80 με)

(3) Damage stage

The pseudostrain in the damage stage was formulated based on Equations 1, 12 and 14:

$$\begin{aligned}\varepsilon_R(t) &= \frac{\sigma_{VE}(t)}{E_R} \\ &= \frac{\varepsilon_0 E(t) - \varepsilon_0 \left|E^*\right|_{LVE} \cos(\omega t - \varphi_D + \varphi_{LVE})}{\left|E^*\right|_{LVE}} \\ &= \frac{\varepsilon_0\left(\left|E^*\right|_{LVE} - \frac{\sigma_{s,LVE}(t)}{\varepsilon_{0,LVE}}\right) - \varepsilon_0 \left|E^*\right|_{LVE} \cos(\omega t - \varphi_D + \varphi_{LVE})}{\left|E^*\right|_{LVE}} \\ &= \varepsilon_0\left[1 - \cos(\omega t - \varphi_D + \varphi_{LVE})\right] - \frac{\varepsilon_0}{\varepsilon_{0,LVE}} \cdot \frac{\sigma_{s,LVE}(t)}{\left|E^*\right|_{LVE}}\end{aligned} \tag{20}$$

For the Nth loading cycle of an RDT test in the damage stage, the pseudostrain was formulated as:

$$\varepsilon_{RN}(t) = \varepsilon_0\left[1 - \cos(\omega t - \varphi_D + \varphi_{LVE})\right] - \frac{\varepsilon_0}{\varepsilon_{0,LVE}} \cdot \frac{\sigma_{sN,LVE}}{\left|E^*\right|_{LVE}} \tag{21}$$

When comparing Equation 5 to Equation 21, it was obviously concluded that $\varepsilon_R(t)$ was out of phase with $\sigma_m(t)$ in the damage stage. The phase angle was $(\varphi_D - \varphi_{LVE})$, which was increasing as the number of loading cycles increased in the destructive RDT test. The $\sigma_m(t)$ vs. $\varepsilon_R(t)$ hysteresis loop of any loading cycle also exhibited an ellipse, whose center was not located at the origin either. The area of this ellipse was the DPSE spent for the following purposes:

- Overcoming the nonlinear viscoelastic effect; and
- Developing damages such as cracking and permanent deformation.

Figure 10 shows the $\sigma_m(t)$ vs. $\varepsilon_R(t)$ graph of the 101st loading cycle of the RDT test with a strain level of 200 με in the damage stage.

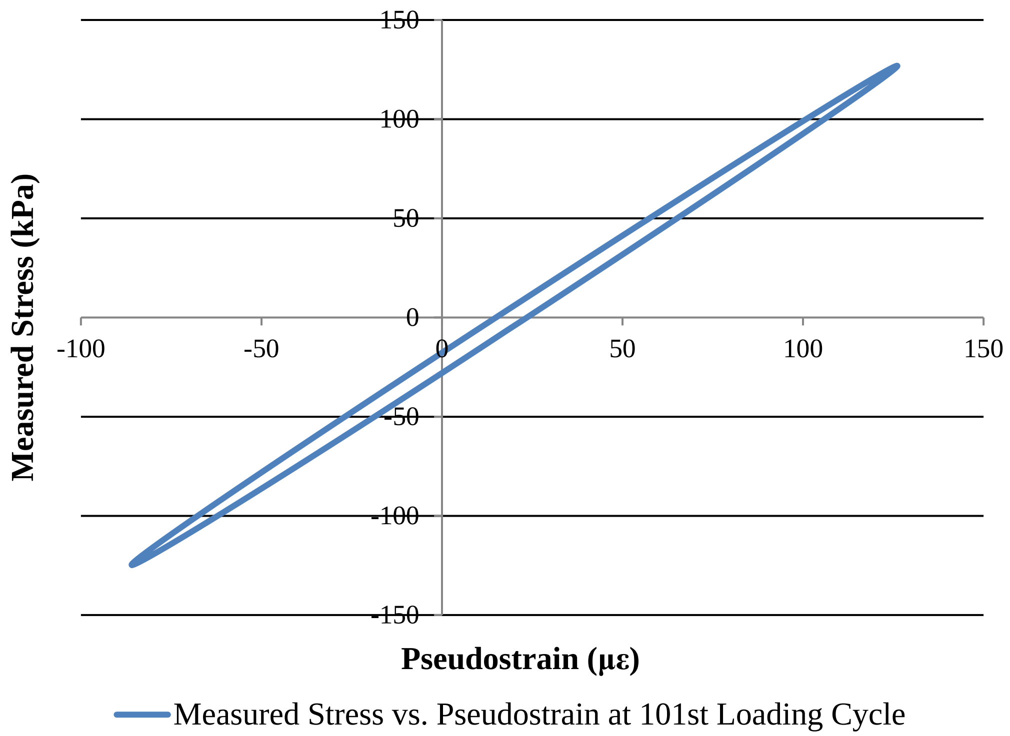

Figure 10 Measured stress vs. pseudostrain in the damage stage
(Strain level = 200 με)

4.3. Dissipated pseudostrain energy (DPSE)

As previously explained, the value of the DPSE was the area of the $\sigma_m(t)$ vs. $\varepsilon_R(t)$ hysteresis loop. The mathematical formulation of the DPSE was shown in Equation 22 [1][2][11][12]:

$$DPSE = \int_{t_1}^{t_2} \sigma_m(t) \frac{\partial \varepsilon_R(t)}{\partial t} dt \tag{22}$$

Based on Equation 22, the DPSEs of representative loading cycles in the linear viscoelastic, nonlinear viscoelastic and damage stages were determined, respectively.

(1) Linear viscoelastic stage

Since the $\sigma_m(t)$ vs. $\varepsilon_R(t)$ hysteresis loop was in fact a straight line, the DPSE in a loading cycle of any RDT test in the linear viscoelastic stage was equal to zero. This fact indicated that there was no DPSE spent overcoming the linear viscoelastic effect.

(2) Nonlinear viscoelastic stage

For any loading cycle in the nonlinear viscoelastic stage, the terms of the integrand in Equation 22, $\sigma_m(t)$ and $\varepsilon_R(t)$, were presented in Equations 5 and 19, respectively. Therefore, the DPSE of a loading cycle in this stage was calculated to be:

$$DPSE = \int_{t_0}^{t_0+\frac{2\pi}{\omega}} \left\{\sigma_{0N}\left[1-\cos(\omega t)\right]-\sigma_{sN}\right\} \frac{\partial \left\{\varepsilon_0\left[1-\cos\left(\omega t-\varphi_{NL}+\varphi_{LVE}\right)\right]-\frac{\varepsilon_0}{\varepsilon_{0,LVE}}\cdot\frac{\sigma_{sN,LVE}}{\left|E^*\right|_{LVE}}\right\}}{\partial t} dt \tag{23}$$

Since $\omega = 2\pi$ rad/s, Equation 23 was simplified to be:

$$DPSE = \pi\sigma_{0N}\varepsilon_0 \sin\left(\varphi_{NL}-\varphi_{LVE}\right) \tag{24}$$

(3) Damage stage

When calculating the DPSE in a complete loading cycle in the damage stage, the formulations of $\sigma_m(t)$ and $\varepsilon_R(t)$ in the integrand in Equation 22 were presented in Equations 5 and 21, respectively. Consequently, the DPSE in a loading cycle in the damage stage was formulated as:

$$DPSE = \int_{t_0}^{t_0+\frac{2\pi}{\omega}} \left\{\sigma_{0N}\left[1-\cos(\omega t)\right]-\sigma_{sN}\right\} \frac{\partial \left\{\varepsilon_0\left[1-\cos\left(\omega t-\varphi_{D}+\varphi_{LVE}\right)\right]-\frac{\varepsilon_0}{\varepsilon_{0,LVE}}\cdot\frac{\sigma_{sN,LVE}}{\left|E^*\right|_{LVE}}\right\}}{\partial t} dt \tag{25}$$

The definite integral was calculated to be:

$$DPSE = \pi\sigma_{0N}\varepsilon_0 \sin\left(\varphi_{D}-\varphi_{LVE}\right) \tag{26}$$

Using Equations 24 and 26, the DPSE of every loading cycle was determined for each RDT test in the nonlinear viscoelastic stage and the damage stage. The determined DPSEs of selected loading cycles in the RDT tests with different strain levels in the nonlinear viscoelastic stage are presented in Figure 11, which demonstrates the following characteristics:

(1) The DPSEs of all loading cycles stayed approximately constant as the number of loading cycles increased; and

(2) When the strain level increased to a higher level within this stage, the DPSE of the loading cycle increased to a larger value.

Figure 12 exhibits the determined DPSEs of loading cycles in the RDT test with a strain level of 200 με, which is in the damage stage. It is clearly illustrated that the DPSE had sustained growth while the number of loading cycles was increasing. This fact indicated that, with the increasing number of loading cycles, an increasing amount of DPSE accumulated to drive the development of damages such as cracking and permanent deformation in the asphalt mixture specimen.

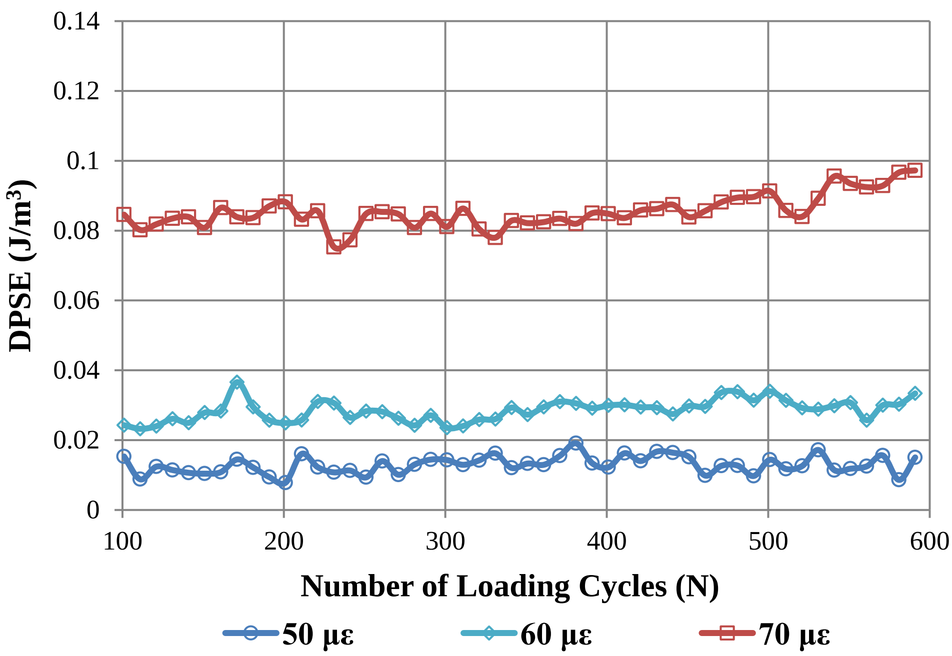

Figure 11 DPSE of loading cycles in RDT tests in nonlinear viscoelastic stage (Strain level = 50, 60, 70 με)

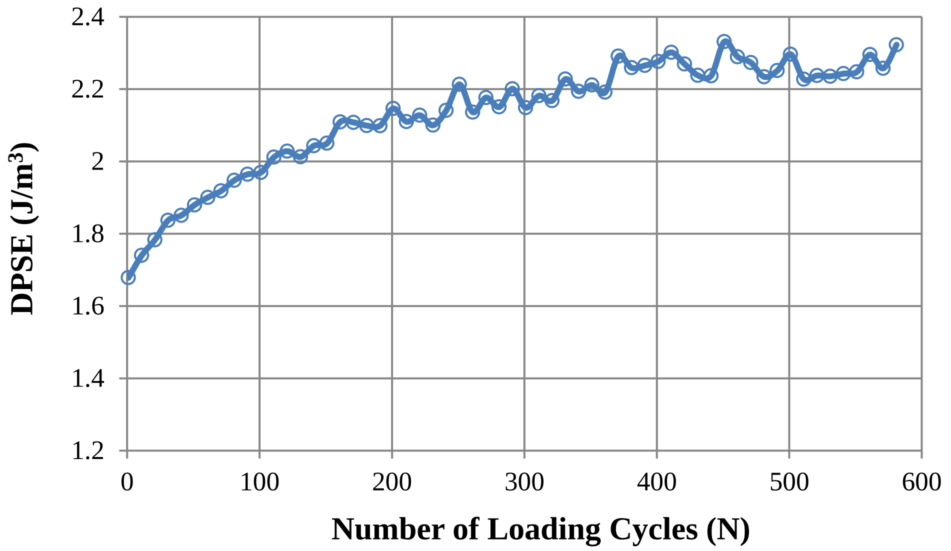

Figure 12 DPSE of loading cycles in an RDT test in damage stage (Strain level = 200 με)

5. Conclusions

This study investigated the material properties of FAM specimens in the linear viscoelastic stage, nonlinear viscoelastic stage and damage stage. These three stages were differentiated and characterized in terms of the viscoelastic stress, pseudostrain and DPSE based on the measurements of controlled-strain RDT tests at a variety of strain levels, which were performed using the DMA. The definitions of viscoelastic stress, reference modulus and pseudostrain were rigorously established in the analysis in order to assure that the material properties in the linear viscoelastic stage were the reference properties. As a result, only the linear viscoelastic effect was eliminated when determining the pseudostrain and DPSE in the three stages. With the successful elimination of the sole linear viscoelastic effect, the measured stress versus pseudostrain in any loading cycle exhibited a straight line passing through the origin in the linear viscoelastic stage but an ellipse-shaped hysteresis loop, whose center was not located at the origin, in both nonlinear viscoelastic stage and damage stage. The area within the hysteresis loop was the DPSE, which was used for different purposes in the nonlinear viscoelastic stage and damage stage:

(1) Nonlinear viscoelastic stage: the DPSE was spent in overcoming the nonlinear viscoelastic effect only; and
(2) Damage stage: the DPSE was spent in overcoming the nonlinear viscoelastic effect and in developing damages such as cracking and permanent deformation in the asphalt mixture.

Based on the formulations of the pseudostrain and DPSE, the DPSEs of all loading cycles were determined for every RDT test at each strain level. The following characteristics of the DPSEs were observed in the three stages:

(1) Linear viscoelastic stage: the DPSE of any loading cycle was zero;

(2) Nonlinear viscoelastic stage:

   a. As the number of loading cycles increased, the DPSE of each loading cycle remained approximately the same, which indicated that the same amount of energy was spent overcoming the nonlinear viscoelasticity in every cycle;

   b. When the strain level of the RDT test increased to a higher level within the nonlinear viscoelastic stage, the DPSE of every loading cycle increased to a larger value and stayed unchanged as the number of loading cycles increased; this fact indicated that more energy was spent overcoming the larger nonlinear viscoelasticity at a higher strain level.

(3) Damage stage: with the growth of the number of loading cycles, the DPSE of the loading cycle was increasing, which indicated that a larger amount of DPSE was spent developing damages including cracking and permanent deformation in the asphalt mixtures.

The findings of this study are capable of strictly differentiating the linear viscoelasticity from the nonlinear viscoelasticity of asphalt mixtures. Therefore, the pseudostrains and the DPSEs of the nonlinear viscoelastic stage and damage stage can be rigorously determined while eliminating the sole linear viscoelastic effect of the asphalt mixtures. This is critical for the accurate determination of the DPSE spent in overcoming the nonlinear viscoelasticity and in developing damages in the asphalt mixtures. The test and analysis methods developed in this study provide clarity, simplicity and accuracy to the characterization of material properties that are used in the design and construction of asphalt pavements. Based on the definitions and formulations established in this study, the DPSE for overcoming the nonlinear viscoelasticity is further distinguished from the DPSE for driving the damage development in an ongoing investigation for the purpose of establishing energy-based models for predicting damage evolution in asphalt mixtures.

Acknowledgements

The authors acknowledge the financial support of the “973 Program” of the Ministry of Science and Technology of China (Project No. 2015CB060100) and the Research Fund for the Doctoral Program of Higher Education of China (Project No. 20120143110004). Special thanks are to the 1,000-Youth Elite Program of China for the start-up funds for purchasing the laboratory equipment that is crucial to this research.

References

[1] Luo, X., Luo, R., and Lytton, R. L. (2013). Characterization of fatigue damage in asphalt mixtures using pseudostrain energy. ASCE *Journal of Materials in Civil Engineering*, 25(2), 208-218.

[2] Luo, X., Luo, R., and Lytton, R. L. (2013). Energy-based mechanistic approach to characterize crack growth of asphalt mixtures. ASCE *Journal of Materials in Civil Engineering*, 25(9), 1198-1208.

[3] Schapery, R. A. (1984). Correspondence principles and a generalized J integral for large deformation and fracture analysis of viscoelastic media. *International Journal of Fracture*, 25(3), 195-223.

[4] Si, Z., Little, D. N., and Lytton, R. L. (2002). Characterization of microdamage and healing of asphalt concrete mixtures. ASCE *Journal of Materials in Civil Engineering*, 14(6), 461-470.

[5] Masad, E., Castelo Branco, V. T. F., Little, D. N., and Lytton, R. L. (2008). A unified method for the analysis of controlled-strain and controlled-stress fatigue testing. *International Journal of Pavement Engineering*, 9(4), 233-246.

[6] Zollinger, C. J. (2005). Application of surface energy measurements to evaluate moisture susceptibility of asphalt and aggregates. Master of Science, thesis, Texas A&M University.

[7] Masad, E., Castelo Branco, V. T. F., Little, D. N., and Lytton, R. L. (2006). An improved method for the dynamic mechanical analysis of fatigue failure of sand asphalt mixtures. Federal Highway Administration, Texas Transportation Institute, Texas A&M University, FHWA/473630.

[8] Vasconcelos, K. L., Bhasin, A., Little, D. N. and Lytton, R. L. (2010). Experimental measurement of water diffusion through fine aggregate mixtures. ASCE *Journal of Materials in Civil Engineering*, 23(4), 445-452.

[9] Tong, Y., Luo, R., and Lytton, R. L. (2015). Moisture and aging damage evaluation of asphalt mixtures using the repeated direct tensional test method. *International Journal of Pavement Engineering*, 16(5), 397-410.

[10] *MATLAB* [computer software]. Math Works, Natick, MA.

[11] Zhang, Y., Luo, R., and Lytton, R. L. (2013). Mechanistic modeling of fracture in asphalt mixtures under compressive loading. ASCE *Journal of Materials in Civil Engineering*, 25(9), 1189-1197.

[12] Zhang, Y., Luo, R., and Lytton, R. L. (2014). Anisotropic characterization of crack growth in the tertiary flow of asphalt mixtures in compression. ASCE *Journal of Engineering Mechanics*, 140(6), 682-694.

[13] Ferry, J. D. (1980). *Viscoelastic properties of polymers*, 3rd edition, Wiley, New York, USA.

[14] Findley, W. N., Lai, J. S., and Onaran, K. (1989). *Creep and relaxation of nonlinear viscoelastic materials: with an introduction to linear viscoelasticity*. Dove Publications, Mineola, New York, USA.

[15] Wineman, A.S., and Rajagopal, K. R. (2000). *Mechanical response of polymers: Introduction*. Cambridge University Press, Cambridge, UK.

Appendix: Derivation of Equation 8

For a sinusoidal strain history $\varepsilon_2(t)=\varepsilon_0\cos(\omega t-\varphi_m)$, the corresponding viscoelastic stress $\sigma_{VE2}(t)$ is derived as follows.

$$\begin{aligned}\sigma_{VE2}(t) &= \int_0^t E(t-\tau)\frac{\partial\varepsilon_2(\tau)}{\partial\tau}d\tau \\ &= \int_0^t E(t-\tau)\frac{\partial\varepsilon_0\cos(\omega\tau-\varphi)}{\partial\tau}d\tau \\ &= -\varepsilon_0\omega\int_0^t E(t-\tau)\sin(\omega\tau-\varphi)d\tau\end{aligned} \tag{A.1}$$

Let $\xi=t-\tau$, then $\tau=t-\xi$, and when $\tau\in[0,t]$, $\xi\in[t,0]$. Equation A.1 is then re-arranged as:

$$\begin{aligned}\sigma_{VE2}(t) &= -\varepsilon_0\omega\int_0^t E(\xi)\sin\left[\omega(t-\xi)-\varphi\right]d(t-\xi) \\ &= \varepsilon_0\omega\int_t^0 E(\xi)\sin\left[(\omega t-\varphi)-\omega\xi\right]d\xi \\ &= \varepsilon_0\omega\int_0^t E(\xi)\left[\sin(\omega\xi)\cos(\omega t-\varphi)-\cos(\omega\xi)\sin(\omega t-\varphi)\right]d\xi \\ &= \varepsilon_0\omega\left[\int_0^t E(\xi)\sin(\omega\xi)d\xi\right]\cos(\omega t-\varphi)-\varepsilon_0\omega\left[\int_0^t E(\xi)\cos(\omega\xi)d\xi\right]\sin(\omega t-\varphi)\end{aligned} \tag{A.2}$$

According to the linear viscoelastic theory [13]–[15], the storage modulus $E'(\omega)$ and the loss modulus $E''(\omega)$ of the complex modulus $E^*(\omega)$ can be expressed as follows:

$$E'(\omega) = \omega\int_0^t E(\xi)\sin(\omega\xi)d\xi = \left|E^*\right|_{LVE} \cos\varphi_{LVE} \tag{A.3}$$

$$E''(\omega) = \omega\int_0^t E(\xi)\cos(\omega\xi)d\xi = \left|E^*\right|_{LVE} \sin\varphi_{LVE} \tag{A.4}$$

Therefore, Equation A.2 is further formulated as:

$$\begin{aligned}\sigma_{VE2}(t) &= \varepsilon_0 E'(\omega)\cos(\omega t-\varphi) - \varepsilon_0 E''(\omega)\sin(\omega t-\varphi)\\ &= \varepsilon_0\left|E^*\right|_{LVE}\cos\varphi_{LVE}\cos(\omega t-\varphi) - \varepsilon_0\left|E^*\right|_{LVE}\sin\varphi_{LVE}\sin(\omega t-\varphi)\\ &= \varepsilon_0\left|E^*\right|_{LVE}\left[\cos\varphi_{LVE}\cos(\omega t-\varphi) - \sin\varphi_{LVE}\sin(\omega t-\varphi)\right]\\ &= \varepsilon_0\left|E^*\right|_{LVE}\cos(\omega t-\varphi+\varphi_{LVE})\end{aligned} \tag{A.5}$$

To summarize, the viscoelastic stress $\sigma_{VE2}(t)$ corresponding to the strain history $\varepsilon_2(t)=\varepsilon_0\cos(\omega t-\varphi_m)$ is determined to be:

$$\sigma_{VE2}(t) = \varepsilon_0\left|E^*\right|_{LVE}\cos(\omega t-\varphi+\varphi_{LVE}) \tag{A.6}$$